

Numerical Predictions on the Intermittent Combustion Instability: Implications and Applications

Shivangi Dhawan¹, Eshaan Raj², Vinayak Malhotra^{3*}

^{1,2}Students, Department of Aerospace Engineering,
SRM Institute of Science and Technology, Kattankulathur, Chennai, India, 603203

^{3*}Assistant Professor & Corresponding Author
Department of Aerospace Engineering,
SRM Institute of Science and Technology, Kattankulathur, Chennai, India, 603203

Abstract

Any application employing combustion places a huge emphasis on safe and effective operations. Several industries make use of relatively small amounts of propellant volumes to generate enormous amounts of energy. For instance, the Aerospace industry requires fuel injection in liquid rocket engines and gas turbine engines for producing thrust. For such cases, combustion comes with its own set of challenges. The predominant challenge among them all is that of combustion instability. Instabilities are physical phenomena occurring in both reacting and non-reacting flows. In the context of engine combustion, they tend to emanate from very small perturbations in the flow field and amplify in magnitude to alter the macroscopic properties of the flow causing problems for the smooth functioning of engines. Since the problem of combustion instability arises from the point of fuel injection itself, this project aimed to look at instability from the viewpoint of intermittent instability in the temporal domain and has redefined it from the perspective of energy loss. For understanding the results in a simplified form, a new zonal system '*i-SEV*' was established. Owing to the heterogeneous heat and mass transfer, optimization and characterization of combustion performance were carried out parametrically to arrive at a conclusive decision of the key parameters in combustion instability and the governing physics behind it.

Introduction

The discovery of fire by humans millions of years ago gave rise to a new era. It not only protected them against predators but also made daily life processes simpler. Soon we realized that fire has way more potential than just being used for cooking. It is a state of ignition, which when initiated is self-sustaining and generates high temperatures and heat. Combustion is the action or process of burning during which a substance undergoes oxidation with the evolution of heat. Combustion in fires is usually incomplete and inefficient, producing less heat, characteristic yellow flames, and a wide range of by-products. While fires are natural and directionless, combustion is desired and plays an active role in several industries, may it be aerospace, medical, or power generation due to which stability in combustion is of primary importance. In terms of thermodynamics, a system is said to be stable when it is in a minimum energy state. Otherwise, the system is considered unstable. The instability in combustion can arise due to very small perturbations

and can magnify further. It deals with irregular heat transfer or uneven heating in the temporal domain. Annually, fire accidents cause thousands of deaths and property damage of more than a billion (Figures 1 & 2). So, it is important to develop a deeper understanding of the instabilities of combustion. Instabilities can appear in different forms and can be broadly be classified into three categories: Intrinsic instability, Combustor instability, and System instability. Intrinsic instability arises due to changes in the flame itself while the combustor instability is caused due to perturbations in a chamber like the coupling of flame with acoustics in the combustor. System instability deals with the supply mechanism of a system and its surrounding. This document primarily talks about system instability as this type of instability is always accompanied by the other two forms. A spray burner (Figure 3) has been considered as the system during the study as an example because it would act as a model for several other real-life scenarios.



Figure 1. Aircraft accident due to plane fire in Moscow (**telegraph.co.uk*).



Figure 2. Destruction due to wildfires in Northern California (**nypost.com*).

Appreciable research efforts have been carried out and reviews of them can be found in [1]-[9]. In 2001, a combustion and radiation model for large-scale fire simulation was developed [1] and different numerical models for the handling of combustion and fire in FDS were made [4]. The studies concluded that the newer version of FDS had improved algorithms in the numerical model than the previous versions for reducing the compilation time by 15% and had also introduced a new method to accommodate under-ventilated fires. During an experimental verification of the FDS Hydrodynamic model, saltwater experiments were performed [3]. DNS is unable to capture the turbulent entrainment in the saltwater plume and LES is preferred over DNS for crude grid resolution [6]. Cheong [4] et. al., carried out investigation and predictions were made by FDS for the heat release rate in a tunnel fire. The estimated results for fire growth were found to be reasonable as similar growth rates and peak HRR were obtained. The use of FDS was considered fairly convenient because parameters apart from the original ones could also be studied.

An attempt to establish goals and structure for Virtual Fire and Smoke Simulation Team/project. The study was successful in establishing the Fire and Smoke Simulation Virtual Research Community for solving complex fire scenarios on robust high-performance computing infrastructure [5]. In a study performed by Kelsey et. al., [6], a large-scale ignition of Liquefied Natural Gas was made onto the surface of a water pool.

Due to the large fire diameter, it was observed that the flames did not cover the entire spill and the flame height was much higher than expected. Although much research has been done to study combustion instability, the driving mechanisms of the instability are still unknown. Having insufficient knowledge of the triggers of the instability is what makes its research even more substantial as the occurrence of these events is increasing perpetually. In a vision of this, a numerical study has been performed on the intermittent combustion instability to understand its implications and applications in a system (Spray Burner) and to study the role of different key parameters in combustion instability, and to figure out a relation between them. In recently, Kevin and Glenn [7], reiterated modulations in the form of ‘*Fire Dynamics Simulator User’s Guide*’, Sixth Edition, 2021.

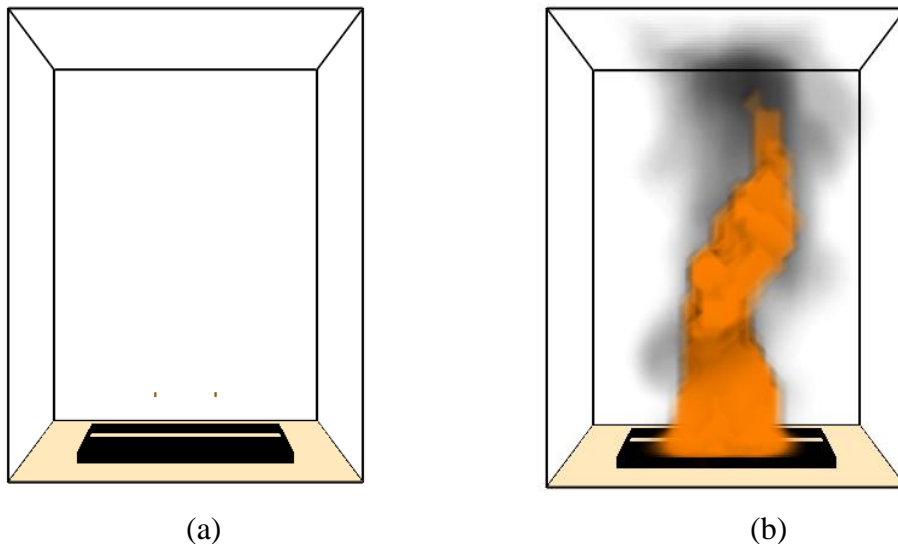


Figure 3. (a), (b) Schematic of the simulated spray burner on FDS.

Numerical Simulation and Methodology

The fundamental conservation equation for fluid dynamics, heat transfer, and combustion were written way before. Applying this conservation equation in a real scenario gives a complex high order differential equation whose analytical solutions were hard to drive. CFD (Computational Fluid Dynamics) models were introduced to solve this complex differential equation by numerical methods. These models have reached a significant development and relatively widespread use in various fields of human activity. Several advanced CFD models for simulation of combustion processes have been developed (e.g., CFX, PHOENICS, and SMART FIRE systems). But for our research, we use Fire Dynamics Simulator (FDS). Fire Dynamics Simulator is a computational fluid dynamics model to simulate low speed ($Mach < 0.3$) fire-driven fluid flow. Its code was written in C and FORTRAN as a programming language. It is developed by the National Institute of Standards and Technology (NIST) of the United States Department of Commerce, in cooperation with the VTT Technical Research Centre of Finland. It uses LES (Large Eddy Simulation) to simulate explicit, second-order, kinetic-energy-conserving numeric or turbulence. Meshes

are usually structured, uniform, staggered grids. In FDS, the Simple immersed boundary method is used for flow obstructions.

To make computation easy, Constant turbulent Schmidt and Prandtl numbers are used. In some places or models generalized “lumped species” methods are used for easy computation of transient analysis. Eddy dissipation concept is taken into account for a single-step chemical reaction between fuel and oxidizer. The governing equations used in the FDS models are the Mass and species transport equation, momentum and energy, and conservation equation. For the hydrodynamic model, the Navier stokes equation is used and solved by LES. For combustion and radiation Mass and species transport equations are used and solved by FVM (Finite Volume Method). While FDS performs analysis, its results are shown in Smokeview (SMV), a tool for visualizing the numerical predictions. It models fire phenomena in a time domain and presents the data through contours and vector plots which are both static and dynamic.

1. Mass and Species Transport:

Fire is a very inefficient combustion process as it involves multiple gases and products species. Track of all these species in the simulation is very difficult. However, to make these species tractable, we limit the number of fuels to one and reaction to one or two. For this, we have to at least keep track of six gas species (Fuel, O₂, CO₂, H₂O, CO, N₂) and one soot particle. For a single-step reaction, we have to solve seven transport equations explicitly. By further assumption, we need to solve two transport equations. One for fuel and another one for products. The air is neither fuel nor product. Fuel is taken as single gas species while the air and products are taken as “lumped species”. The mass transport equations make no distinction between a single or lumped species. The required transport equation is:

Where Z denotes the mass fraction, \dot{m} denotes the production rate and D denotes the diffusive flux of

$$\frac{\partial}{\partial t}(\rho Z_{\alpha}) + \nabla \cdot (\rho Z_{\alpha} \mathbf{u}) = \nabla \cdot (\rho D_{\alpha} \nabla Z_{\alpha}) + \dot{m}_{\alpha}''' + \dot{m}_{b,\alpha}'''$$

species α . ρ denotes the mass density. \mathbf{u} is velocity. The species transport equations are solved using a predictor-corrector scheme. Advection terms are written in flux divergence (conservative) form. In the predictor step, the mass density in cell ijk at time level $n+1$ is estimated based on information at the n th level.

2. Momentum Transport:

Momentum transport deals with the transport of momentum which is responsible for flow in fluids. It also describes the science of fluid flow also called fluid dynamics. The governing equation that deals with the momentum transport in the fluid are the Navier-stokes equation. FDS solve the Navier-stokes equations numerically which are appropriate for low speed, thermally driven flow with an emphasis on smoke and heat transport from fire. The core algorithm for this equation is an explicit predictor-corrector scheme which is second-order accurate in space and time. Large Eddy Simulation (LES) is used for the simulation of turbulence models. It is also possible to perform the Direct Numerical Simulation (DNS) if the meshes are fine enough. The momentum equation can be written as:

Where ‘ f_b ’ denotes the drag force exerted by the sub grid-scale particles and droplets. H denotes stagnation

$$\frac{\partial \mathbf{u}}{\partial t} - \mathbf{u} \times \boldsymbol{\omega} + \nabla H - \tilde{p} \nabla (1/\rho) = \frac{1}{\rho} \left[(\rho - \rho_0) \mathbf{g} + \mathbf{f}_b + \nabla \cdot \boldsymbol{\tau} \right]$$

energy per unit mass and $\boldsymbol{\tau}$ denotes viscous stress. \tilde{p} denotes perturbation pressure.

3. Energy Transport:

Energy transport deals with the transport of different forms of energy in a system and is also known as heat transfer. In the energy transport equation, combustion and radiation are included by the source terms present in the governing equation. FDS solves the combustion model by using a single step, a mixing-controlled chemical reaction that uses three lumped species (fuel, air, and products). Fuel and products are computed explicitly. Radiative heat transfer is computed in the model by the solution of the radiation transport equation for a grey gas and in some limited cases, a wideband model is also used. This equation is solved by the Finite Volume Method (FVM). The absorption coefficients of the gas-soot mixtures are computed using the RadCal narrow-band model. The absorption and scattering coefficients are based on Mie theory. As the problem of combustion instability arises from the point of fuel injection, an example of a spray burner is taken in the FDS. In the example file (Spray Bburner), heptane from two nozzles is sprayed downwards into a steel pan. The flow rate is increased linearly so that the fire grows to 2 MW in 20 s, burns steadily for another 20 s, and then ramps down linearly in 20 s. The density of the heptane is taken as 684 kg/m^3 . The heat of combustion for this whole reaction is taken as 44500 KJ/Kg. The parameters of the spray burner are varied linearly and then their variation is noted in the temporal domain with respect to the base value. The parameters which are varied in this example are Spray Angle, Particle Velocity, and Flow Rate. The base value for the spray angle, particle velocity, and flow rate is 45 degrees, 10 m/s, and 1.97 L/min respectively. In the spray burner, 2 MW is achieved via two nozzles flowing the heptane at 1.97 L/min each:

$$2 \times 1.97 \text{ L/min} \times 1/60 \text{ min/s} \times 684 \text{ kg/m}^3 \times 1/1000 \text{ m}^3/\text{L} \times 44500 \text{ KJ/Kg} = 1998.762 \text{ KW} \approx 2000 \text{ KW}$$

- a) **Spray Angle:** It is the angle at which heptane droplets are sprayed through the nozzle in the steel pan. A total of 5 simulations is done with each having a simulation time of 90 sec. Angles are varied linearly with a uniform difference of 15 degrees. The angles are 15,30,45,60 and 75 degrees. The remaining parameters are kept constant.
- b) **Particle Velocity:** It is the velocity at which particles (heptane droplets) come out from the two nozzles. A total of 5 simulations is done with each having a simulation time of 90 sec. Angles are varied linearly with a uniform difference of 5 m/s. The angles are 10, 15, 20, 25 and 30 m/s. The remaining parameters were kept constant.
- c) **Flow Rate:** It is the net mass flow rate of the fuel(heptane) from the two nozzles in L/min. A total of 5 simulations is done with each having a simulation time of 90 sec. Angles are varied linearly with a uniform difference of 1 L/min. The angles are 1.97, 2.97, 3.97, 4.97 and 5.97 L/min. The base value is 1.97 L/min. The remaining parameters are kept constant.

Results and Discussion

For the validation of the results obtained from the study, the graph for the Gross Heat Release Rate for a Combustion Process has been shown in Figure 4 (a). The simulator predictions match reasonably well with the conventional Heat Transfer theory as GHRR is increasing with time. So, the data from the study is expected to provide good physical insight into the Combustion Instability Phenomenon.

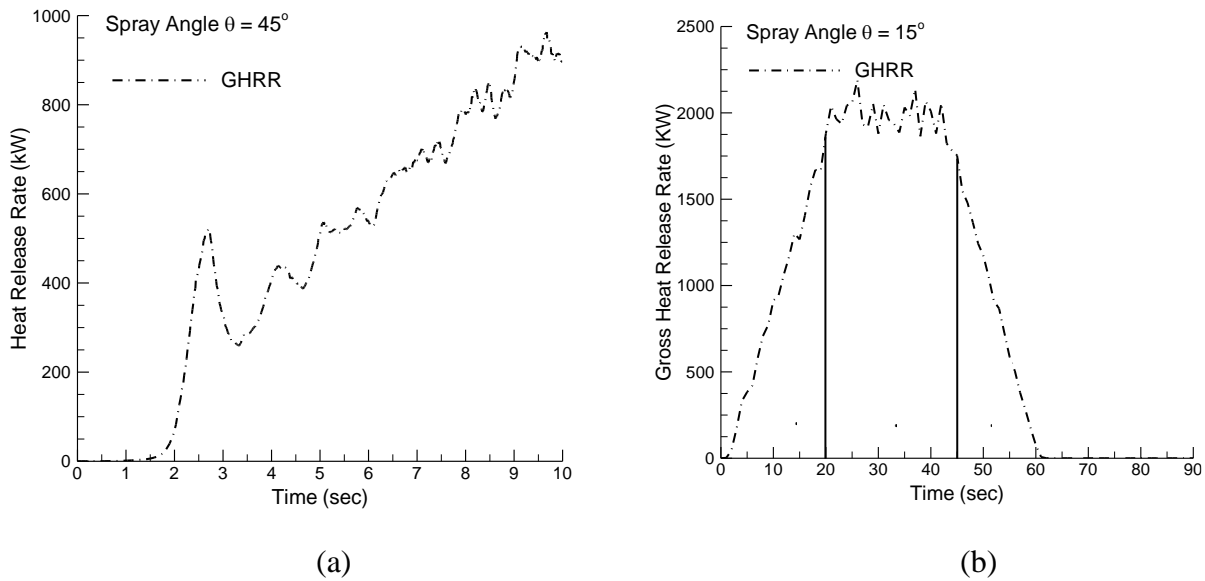


Figure 4. Validation of the Simulation Predictions: (a) Heat Release Rate vs Time (b) Novel zonal system introduced ‘i-SEV zonal system’.

In order to make the understanding of the plots simpler and to organize the instability within a system, a new zonal system has been introduced which would be referred to as ‘i-SEV Zonal System’ in the rest of the document. Its demonstration has been made in figure 4(b) and can be visually categorized into three zones:

- a) **i-SEV 1:** It starts with ignition and continues for a period of 20 seconds. In this zone, the fire is ignited and the flow field propagates until the release rates reach a fairly constant range which is the beginning of zone 2.
- b) **i-SEV 2:** It starts at the end of i-SEV 1 and lasts up to 45 seconds. The significance of this zone is that though the release rates remain in a certain range, the fluctuations are maximum which implies that there could be maximum damage in this zone.
- c) **i-SEV 3:** This is the receding zone that lasts for nearly 15 seconds. The losses decrease in this zone and the system regains stability after the 60-second benchmark.

Figure 5 (a) shows the effect of the variation of spray angle on the Gross Heat Release Rate (GHRR) and the different heat transfer rates over a period of 90 seconds. The y-axis of the plot represents the heat release rates in kilowatts (kW) whereas the x-axis represents time in seconds (sec). It was noted, that though there are minor fluctuations, the five spray angle variations follow the same trend overall with the total HRR nearing 2000 kW. This further validates the i-SEV zonal system as the values of the parameters might vary from system to system but the zones can still be defined qualitatively. It can also be observed from figures 5 ((b), (c), and (d)) which represent radiation, convection, and conduction heat release rates respectively, that the losses through radiation are nearing 750 kW, those through convection reach a maximum of 1400 kW whereas the conduction losses barely cross the 20 kW benchmark.

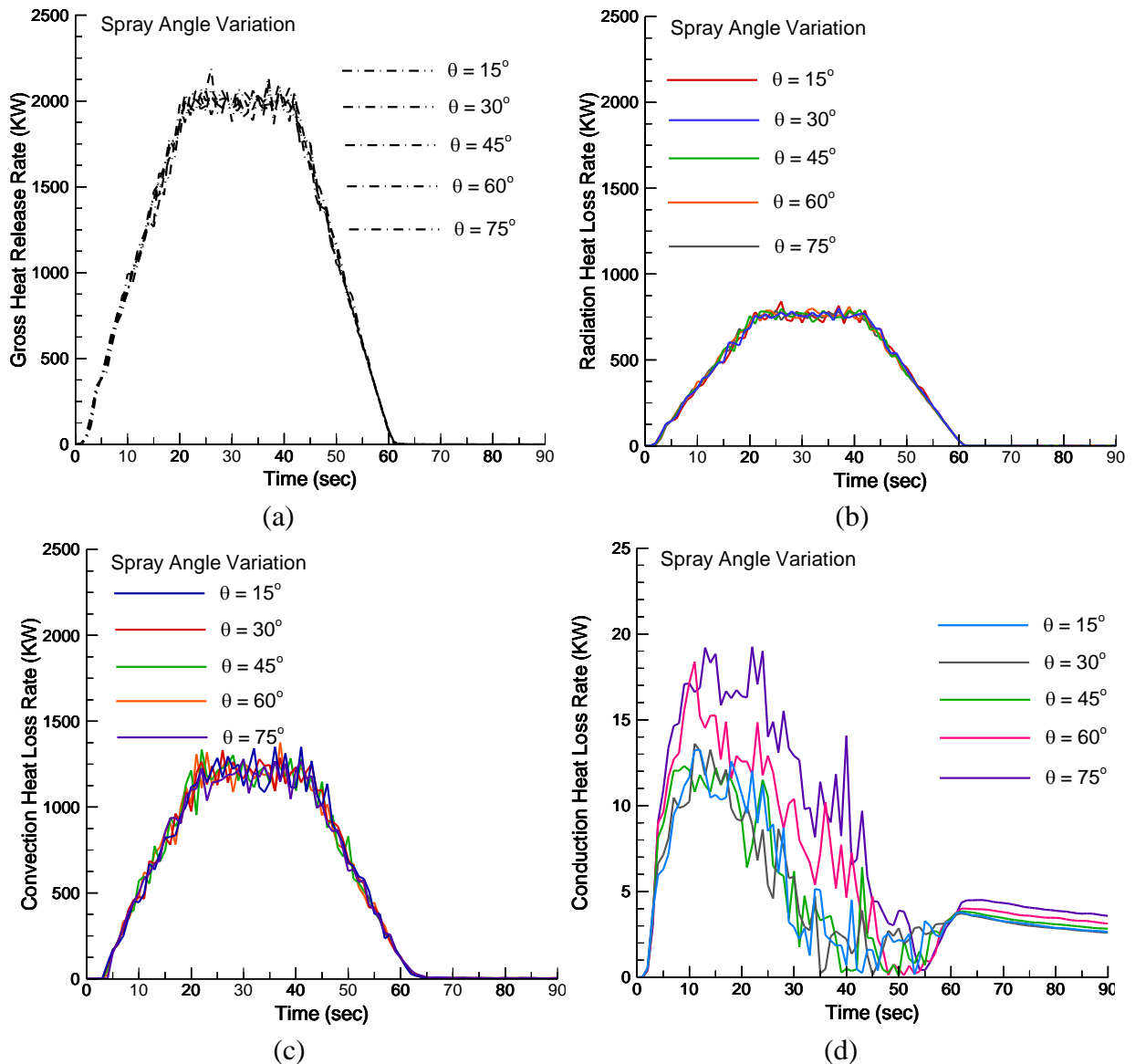


Figure 5. Effect of Spray angle variation (Linear) and Related Heat Transfer Rate(s) in the onset of Combustion Instability, (a) GHRR vs Time, (b) Radiative losses vs Time, (c) Convective losses vs Time, (d) Conductive losses vs Time.

The x-axis of i-SEV did not vary during this analysis despite the changing values in the y-axis. In i-SEV 1, the heat release rates are on a rise with minute fluctuations within the general trend unlike i-SEV 2 where the rates are fairly on the same level with large perturbations. As the system moves in i-SEV 3 the release rates start to fall until it reaches a bare value where the system can be considered stable.

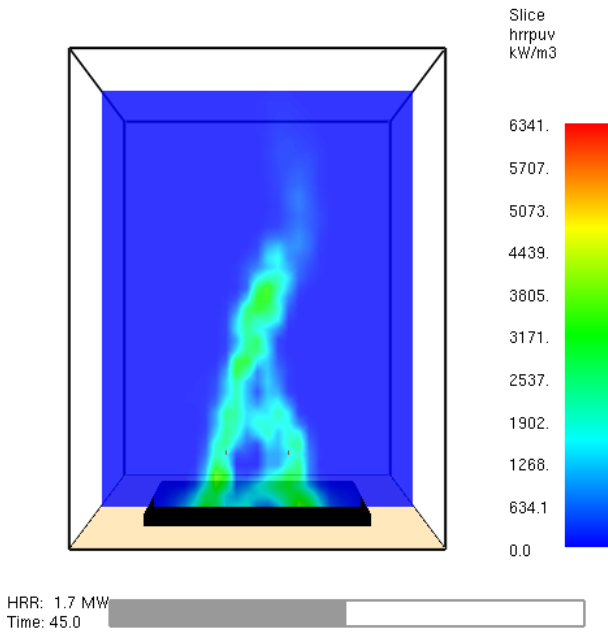


Figure 6. Heat Release Rate contour of spray burner.

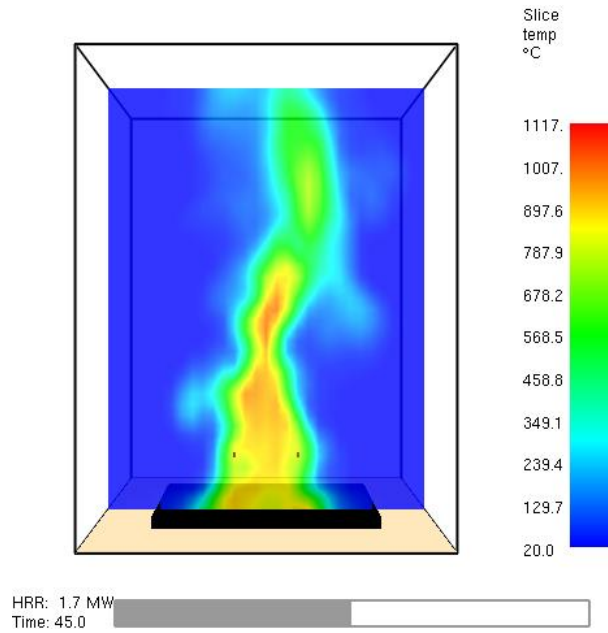


Figure 7. Temperature contour of spray burner.

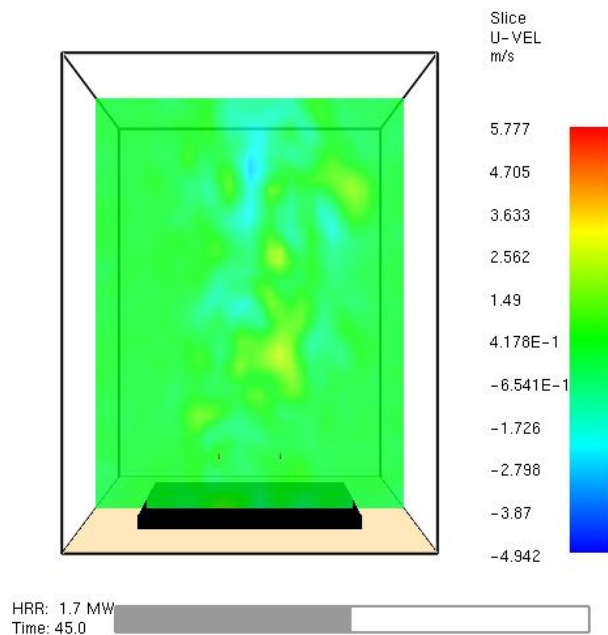


Figure 8. Contour of U-velocity vector of burner.

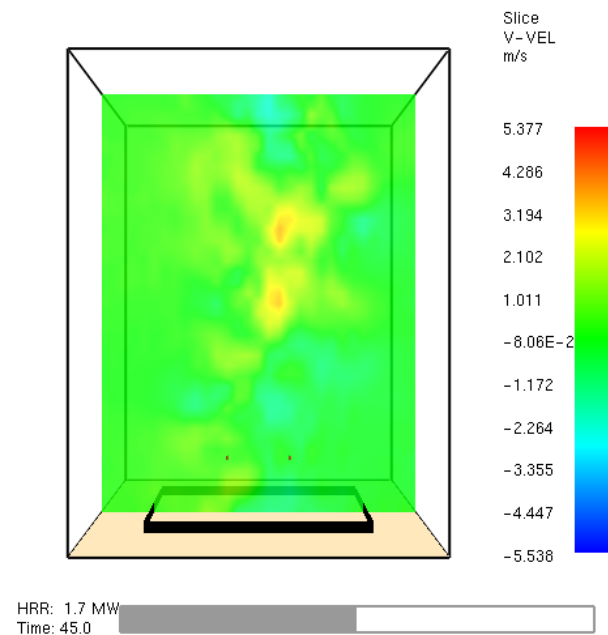


Figure 9. Contour of V-velocity vector of spray burner.

The different contours of spray angle variation for 60 degrees at a time of 45 seconds for heat release rate per unit volume, temperature, and flow velocity in U, V, and W direction are shown in figures 6-10. It was noted that the contours are in resemblance with the plots generated as the flow is highly unstable. The heat release rate per unit volume for the whole experiment remained between 0 and 6341 kW/m³, and the temperatures did not exceed 1117 degrees. The velocity in the U, V, and W direction ranged between -5.538 to 15.21 m/s.

Figures 9 ((b), (c), and (d)), which illustrate radiation, convection, and conduction heat loss rates, show that radiation losses are approaching 750 kW, convection losses peak at 1500 kW, and conduction losses barely exceed the threshold of 25 kW.

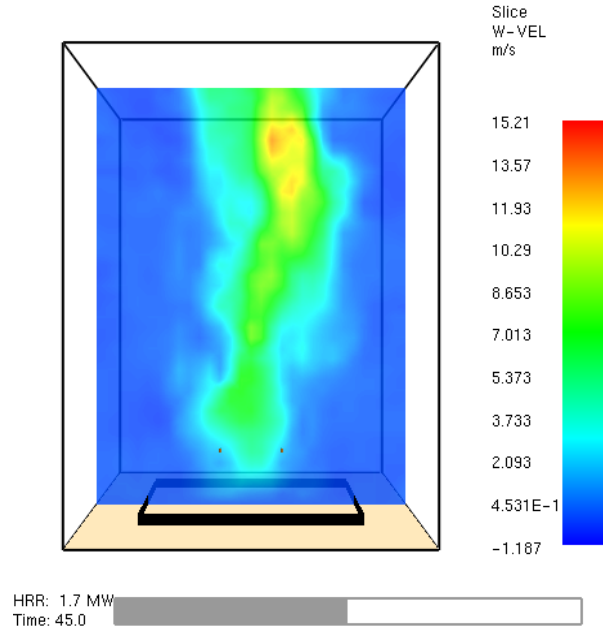


Figure 10. Contour of W-velocity vector of spray burner.

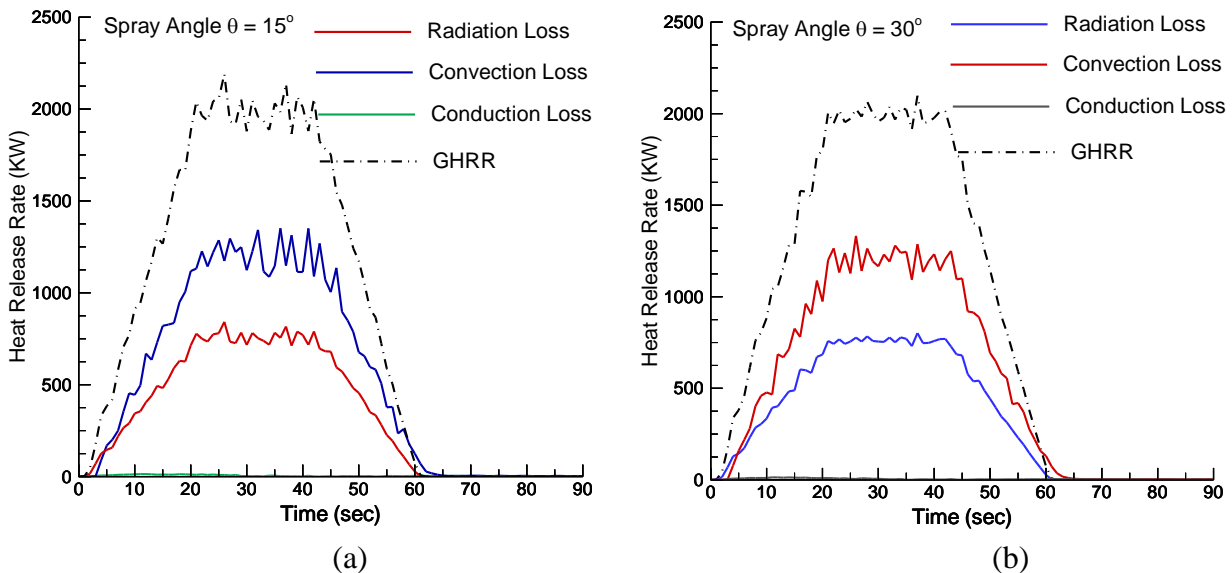


Figure 11 distinguishes the heat release rates and losses for each spray angle variation. It is clear from the graphs that the loss of energy is convection dominant and is driven by radiation. Although losses through conduction are very minute, they persist in all the cases due to which it can be concluded that heat transfer always exists in all three forms. Despite the altering magnitudes of the losses in the system, the x-axis of i-SEV did not change during this study as the parameters were varied linearly. The impact of changing particle or flow velocity on the Gross Heat Release Rate (GHRR) and the various heat transfer rates during a 90-second period is depicted in Figure 12. The plot's y-axis depicts heat release rates in kilowatts (kW), while the x-axis depicts the time in seconds (sec). It should be noticed that, despite slight differences, the

five spray angle modifications all follow the same general pattern, with the total HRR approaching 2000 kW.

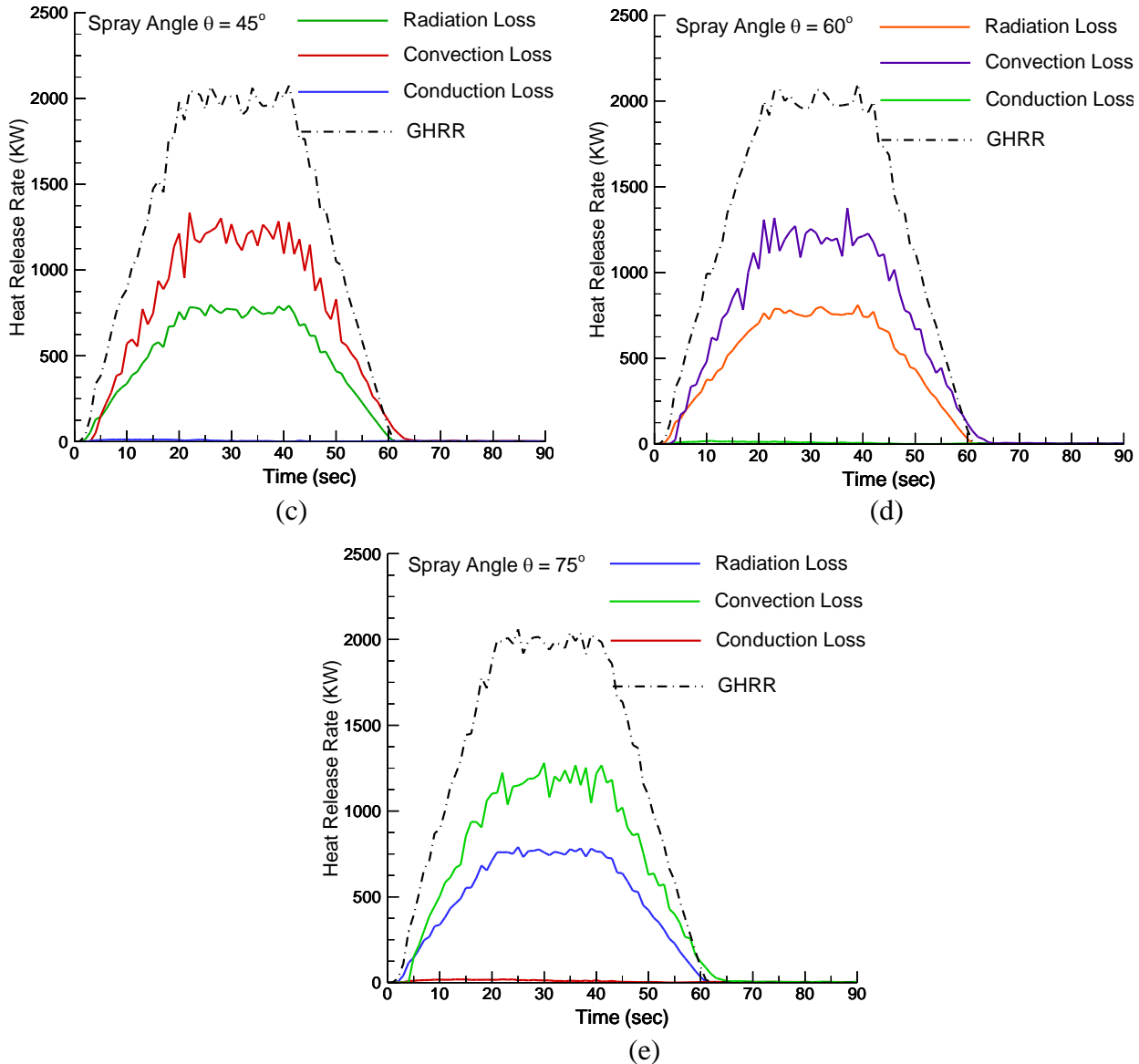


Figure 11. Role of varying heat transfer rates (HRR) on induced combustion instability at different spray burner angles (a) $\theta = 15^\circ$, (b) $\theta = 30^\circ$, (c) $\theta = 45^\circ$, (d) $\theta = 60^\circ$, (e) $\theta = 75^\circ$.

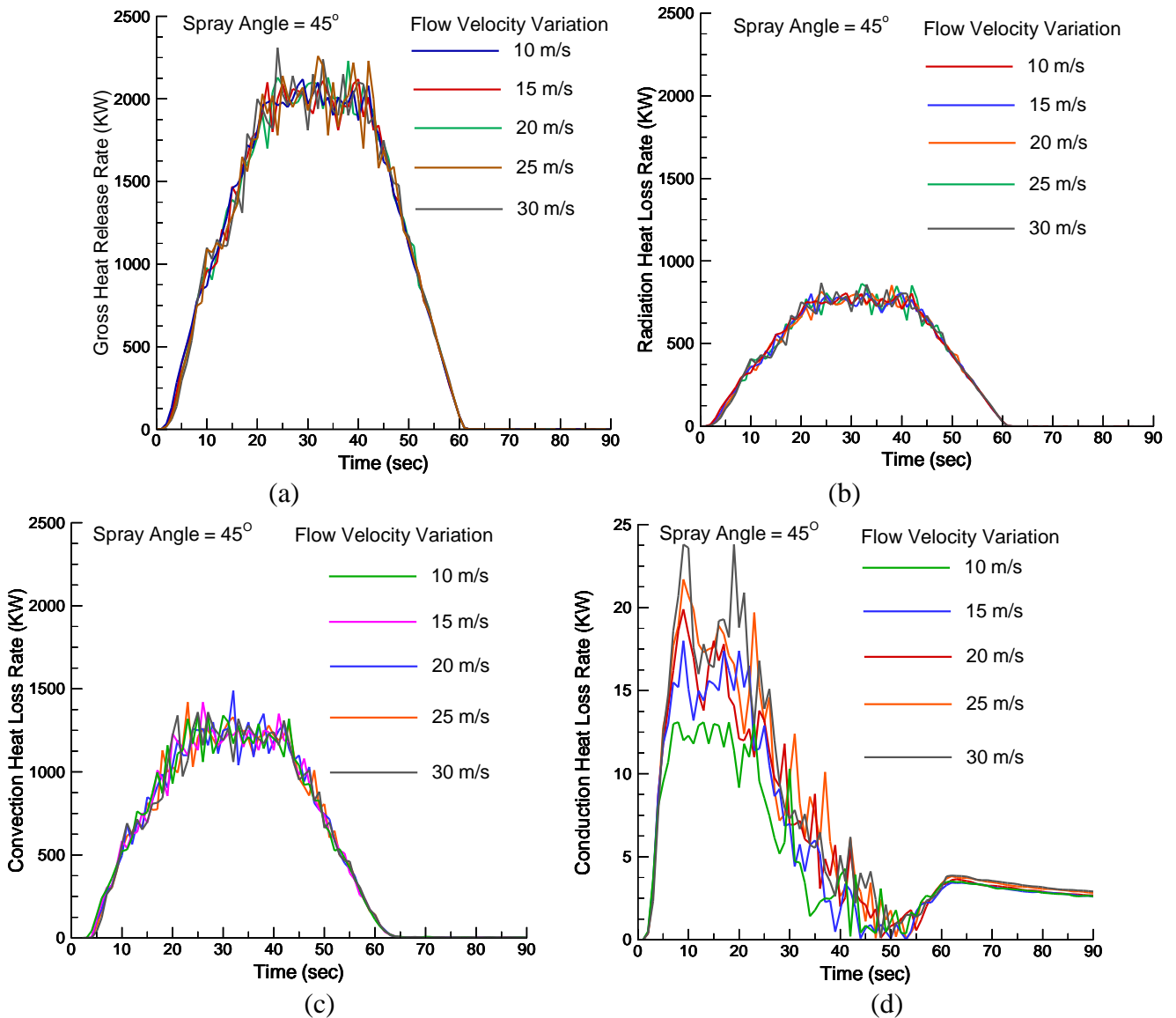


Figure 12. Role of varying energy transfer rates on induced combustion instability at different linear burner flow velocities variation, (a) GHRR, (b) Radiative losses, (c) Conductive losses, (d) Conduction losses.

The vector contours of Heat release rate per unit volume, temperature, and the flow velocity in U, V, and W directions for the particle velocity variation are demonstrated in figures 13-17. The simulation time for all the vector contours was fixed at 45 seconds and the particle velocity at 20 m/s so that they can be compared among themselves and can be related to the plots. The heat release rate per unit volume for the whole experiment remained between 0 and 7929 kW/m³, and the temperatures did not exceed 1128 degrees. The velocity in the U, V, and W direction ranges between -6.083 to 15.24 m/s.

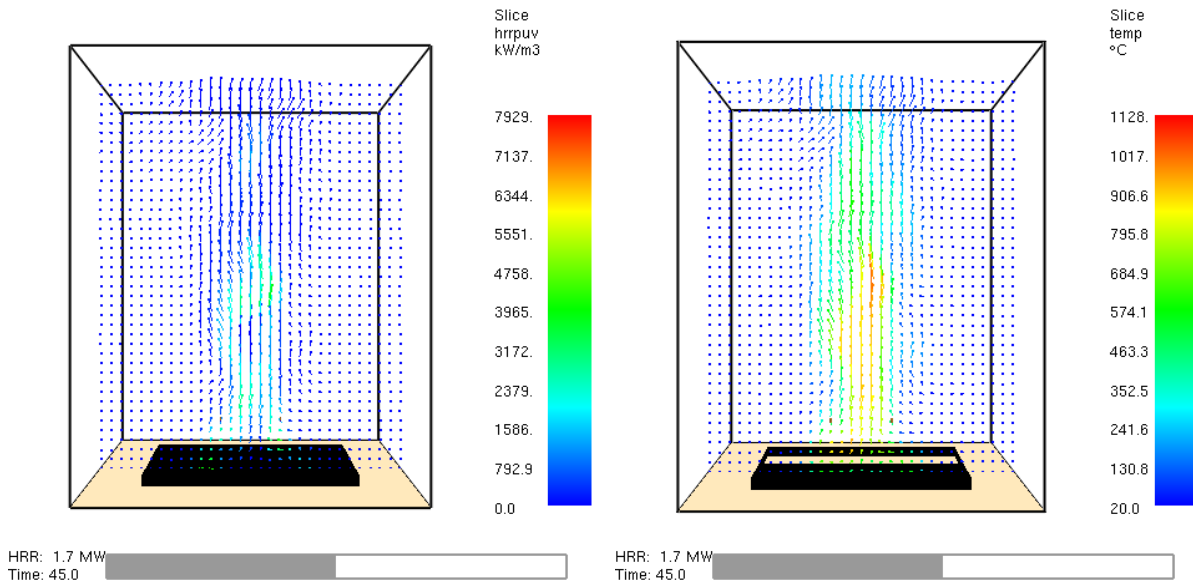


Figure 13. Vectors contour of Heat Release Rate of spray burner.

Figure 14. Vector contour of Temperature of spray burner.

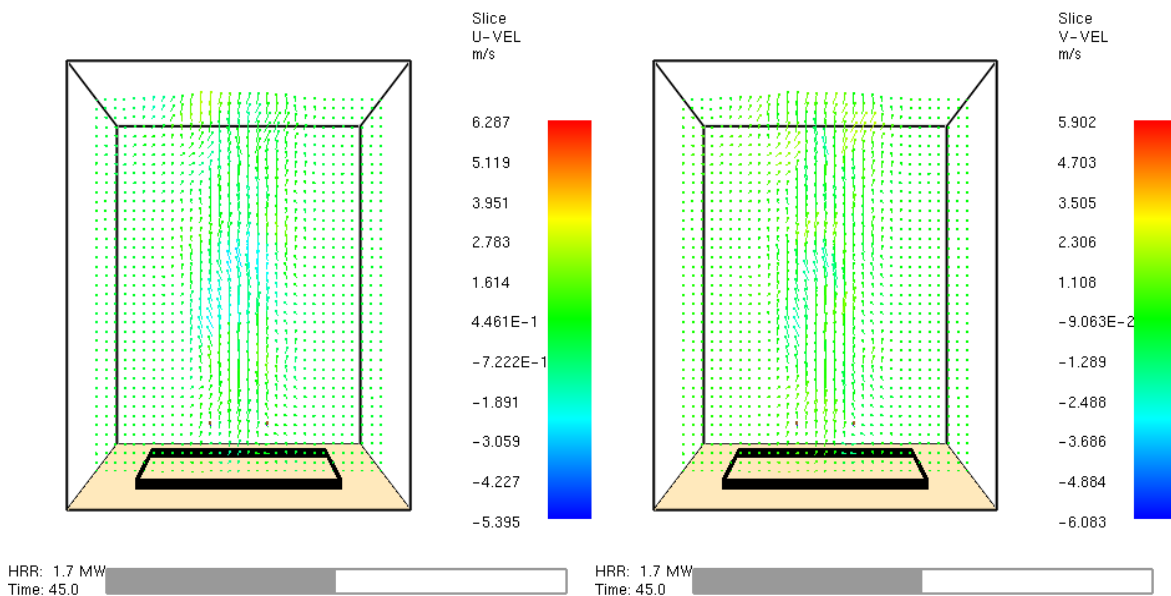


Figure 15. Vector contour of U-velocity vector of spray burner.

Figure 16. Vector contour of V-velocity vector of spray burner.

The heat release rates and losses for each flow velocity variation are shown in Figure 18. The simulation was done while keeping the spray angle at a constant value of 45 degrees. It is clear from the graphs that the maximum loss of energy is through convection followed by radiation. In i-SEV 1, heat release rates are increasing with minor oscillations within the overall trend, but in i-SEV 2, rates are relatively constant with substantial fluctuations. The release rates start to reduce as the system goes through i-SEV 3, until it hits a minimal value at which the system can be regarded as stable.

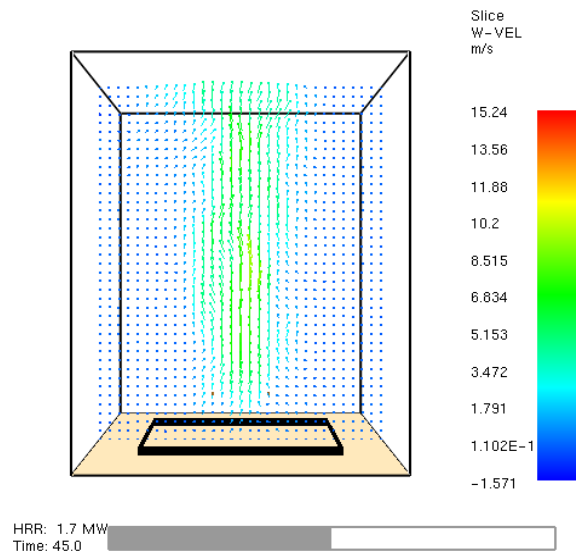
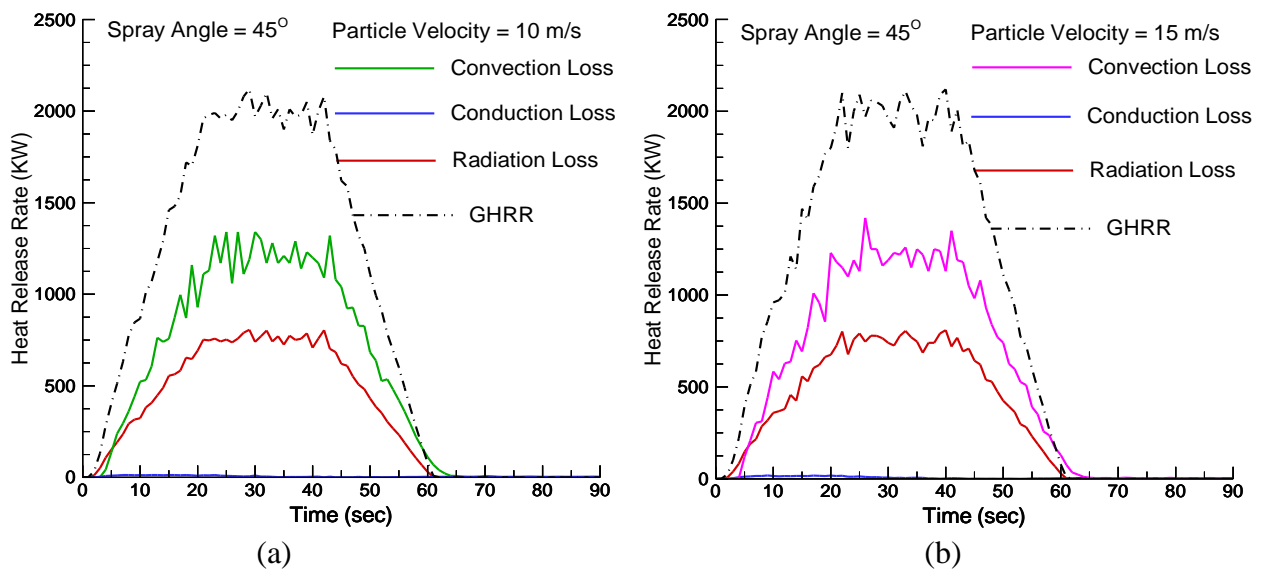


Figure 17. Vector of W-velocity vector of spray burner.



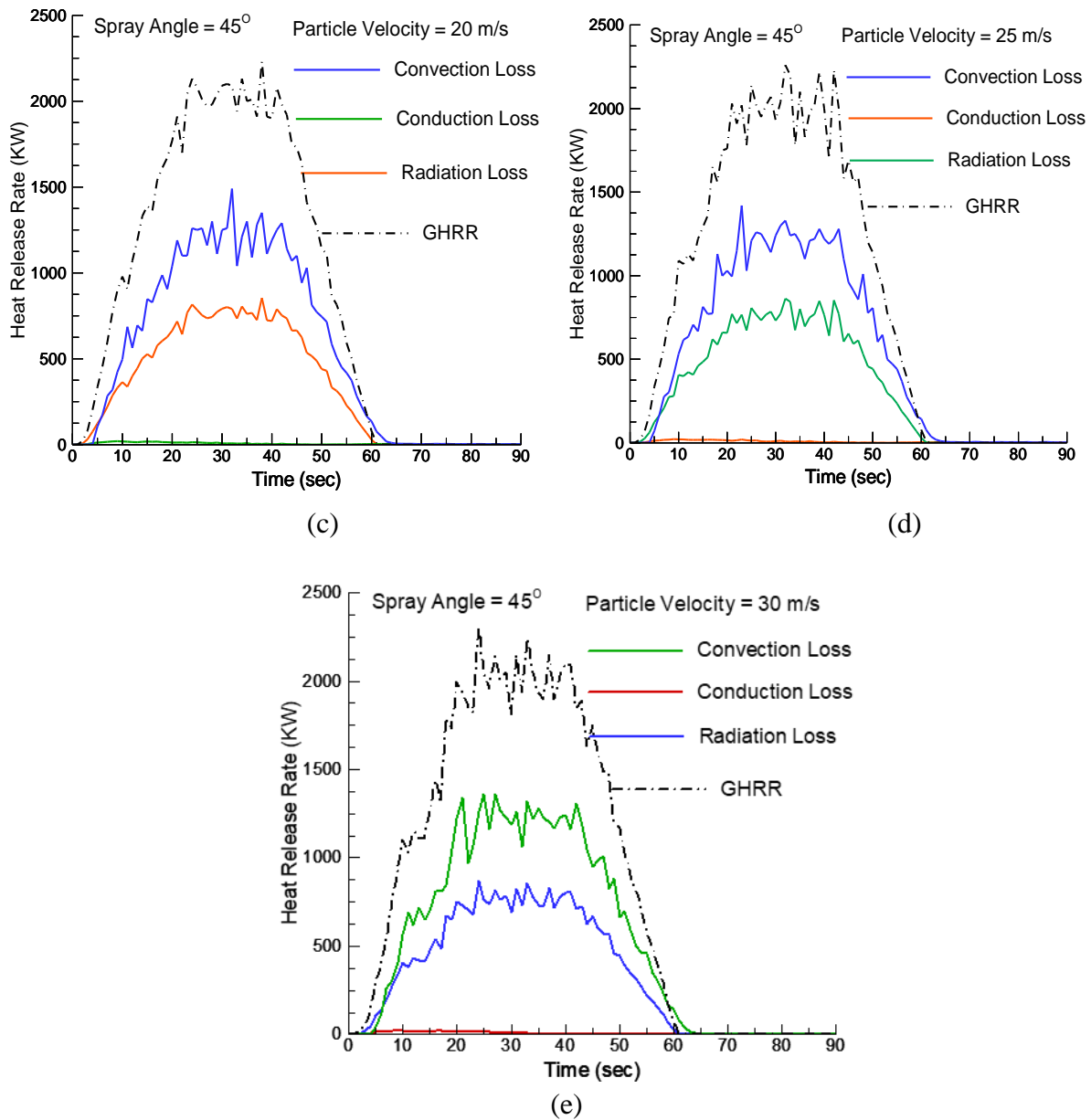


Figure 18. Role of varying heat transfer rates on induced combustion instability at different flow velocities, (a) 10 m/s, (b) 15 m/s, (c) 20 m/s, (d) 25 m/s, (e) 30 m/s.

The simulation results of the flow rate variation are shown in Figure 19. The Gross Heat Release Rate increases with the increase in flow rate while Spray Angle and Particle Velocity were kept constant. It is clear that even with slight changes in the value of flow rate, the heat release rates are increasing significantly which makes the Flow Rate of the propellant a key parameter in combustion instability, i.e., the higher the flow rate the higher will be the losses.

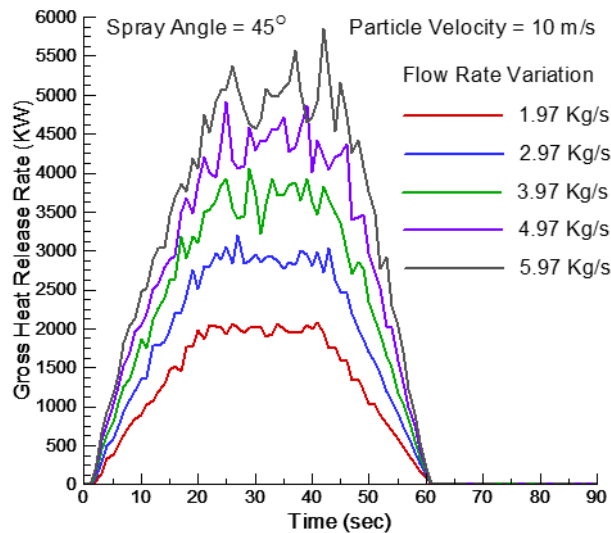


Figure 19. Role of varying heat transfer rates on induced combustion instability at different linear burner flow rate variation.

Conclusion

Having a wide range of applications in aerospace engines, power plants, genetics, and even the food industry, combustion brings along with itself a bunch of problems. To counter the number of mishaps by studying the causes of the instabilities and proposing a redefined version of combustion instability, a calibrated simulation of spray burner experiment using FDS was performed. The results from the simulation demonstrated that the system first becomes unstable, which was explained by introducing a new zonal system “i-SEV”, after which the system regains stability. By using the three zones, we can now define the path of instability that a system would undergo. The heat release rates of the three modes of heat transfer, Conduction, Convection, and Radiation, were defined in terms of losses of the system which were convection dominant and were driven by radiation. Conduction losses were present too but they were very small as compared to the other two. From the parametric analysis, it was found that Flow Rate was a key parameter of the combustion instability. The knowledge of these instabilities can be applied to different applications to predict the path of the instability and the parameters which could affect the system performance so that by knowing which zone the system is under loss of lives and property damage can be reduced.

Applications of the present work: The results presented here cover a wide range of applications like the Aerospace industry, Automobile industry, Power plant, etc. For example, in aerospace industries, the results can be applied to aircraft and rocket engines. They can be used to improve our understanding of combustion instability and help us minimize the losses from fire accidents. The principles can be employed in liquid fuel engine vehicles and in the designing of futuristic vehicles.

References

- [1] McGrattan, K., Floyd, J. E., Forney, G. P., Hostikka, S. A., and Baum, H. R., ‘*Development of Combustion and Radiation Models for Large Scale Fire Simulation*’, Third Technical Symposium on Computer Applications in Fire Protection Engineering, 2001.

- [2] Galea, E R., and Patel, M., '*Principles and Practice of Fire Modelling. A Collection of lecture notes for a short course prepared by the Fire Safety Engineering Group*', CMC Press Publications, Fourth Edition, 2001.
- [3] Clement, J.M. and Fleischmann, C.M., '*Experimental Verification of The Fire Dynamics Simulator Hydrodynamic Model. Fire Safety Science*'. International Association for Fire Safety Science. 7. 839-850. 10.3801/IAFSS.FSS.7-839, 2003.
- [4] Cheong, M.K., Spearpoint, M. J., and Fleischmann, C. M., '*Calibrating an FDS Simulation of Goods-vehicle Fire Growth in a Tunnel Using the Runehamar Experiment*', Journal of Fire Protection Engineering. ;19(3):177-196, 2009.
- [5] Tran, V., '*Tunnel Fire Simulation using FDS (Fire Dynamics Simulator)*', EGI Community Forum 2012 / EMI Second Technical Conference, 155.10.22323/1.162.0155, 2012.
- [6] Kelsey, A., Gant, S., McNally, K., and Betteridge, S., '*Application of global sensitivity analysis to FDS simulations of large LNG fire plumes*', Institution of Chemical Engineers Symposium Series, 2013.
- [7] Kevin M. G., Glenn F, '*Fire Dynamics Simulator User's Guide*', Sixth Edition, 2021.